The concept of frozen elastic energy as a consequence of change in microstructure morphology

Witold Krasny, Claire Morin, Stéphane Avril, Hélène Magoariec, Christian Hellmich

The concept of frozen elastic energy as a consequence of change in microstructure morphology

W. KRASNY[a,b], C. MORIN[a], S.AVRIL[a], H. MAGOARIEC[b], C. HELLMICH[c]

a. Centre for Biomedical and Healthcare Engineering, CNRS UMR 5307 (LGF), Ecole Nationale Supérieure des Mines, Saint-Etienne, France
b. Laboratoire de Tribologie et Dynamique des Systèmes, CNRS UMR 5513, Université de Lyon, Ecole Centrale Lyon, France
c. Institute for Mechanics of Materials and Structures, Vienna University of Technology, Austria

Résumé :

Une approche micromécanique et multi-échelle pour la modélisation des tissus mous explique la non-linéarité de leur réponse au chargement mécanique, la dépendance de leur réponse mécanique vis-à-vis de la trajectoire de déformation ainsi que l'éventuelle énergie stockée, comme conséquences du changement de morphologie de la microstructure.

Abstract :

A micromechanics multi-scale approach to soft tissues modeling explains the non-linearity of their response to mechanical loading, as well as path dependence and possible frozen elastic energy, as a consequence of change in microstructure morphology.

Key words : modeling, multi-scale, microstructure, reorientation

1 Introduction

Soft tissues are biological unmineralized tissues, such as arteries, tendon, or skin, made of variously oriented and crimped elastic and collagen fibers embedded in a soft hydrogel-like matrix. Mechanically, these tissues exhibit a highly non-linear, anisotropic behavior, with the ability to sustain large strains. Modeling this complex constitutive behavior has been the topic of abundant literature, mainly focused on macroscopic, phenomenological, large strain hyperelastic models [2,3,4], inspired from rubber mechanics [5,8,9]. However, the recent development of 3D multiphoton confocal microscopy techniques has open the way to image the collagen and elastic fiber bundles allowing correlation of the highly non-linear behavior of soft tissues with significant microscopic

geometrical rearrangements. In deforming soft tissues, such rearrangements encompass progressive decrimping and realignment of the fibers along the load direction [10]. The pressing need to correctly capture the relations between microscopic mechanisms and macroscopic mechanical response drives forward the development of multiscale approaches [7]. We here propose an explicit consideration of microstructure evolutions of soft tissues through adaptation of the framework of continuum micromechanics [12] and extension of the Eshelby's inclusion problem [1,6]. In particular, we investigate the ability of the proposed model to capture, through microstructure morphology changes, the non-linear mechanical response of soft tissues, the possible path dependence of their response to multiaxial loading, and the presence of a remaining frozen elastic energy after complete unloading.

2 Methods

2.1 Micromechanical representation of soft tissues

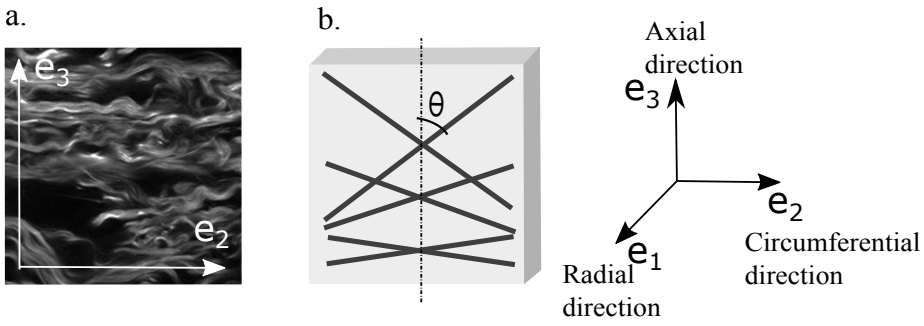

FIGURE 1 – (a) Collagen bundles of unloaded rabbit carotid artery imaged with confocal bi-photon microscope (IVTV Platform, ANR-10-EQPX-06-01, FR) - window size : $250 \times 250\ \mu m$. (b) Associated representative volume element with 6 fiber families showing different fiber orientation angles θ.

Since the model is developed in the framework of continuum micromechanics, we do not resolve each and every detail within the soft tissue microstructure, but we introduce homogeneous subdomains called material phases. Accordingly, we consider a simplified representative volume element (RVE) of a few hundreds micrometer size made of soft tissue material (see Figure 1), which hosts variously oriented, infinitely long fiber-like inclusions (labeled by index f) with a volume fraction f_f, embedded in a matrix (labeled by index m), with a volume fraction $f_m = 1 - f_f$. The six fiber families considered in the present work, with a total volume fraction of $f_f = 0.70$, all belong to the plane $(\boldsymbol{e}_2, \boldsymbol{e}_3)$; their inclination is therefore characterized by only one angle θ, defined as the angle between the axial direction of the artery, $\boldsymbol{e}_3$, and the fiber axis. In this work, the initial inclination of the six fiber families is chosen in the interval $\theta \in [\pi/4; 3\pi/4]$. Each phase i is characterized by a hypoelastic constitutive relation,

reading as :

$$\overset{\triangle}{\boldsymbol{\sigma}}_i = \mathbb{C}_i : \boldsymbol{d_i} \quad (i \in \{f, m\}) \tag{1}$$

In the previous equation, $\mathbb{C}_i$ is the fourth-order stiffness tensor of phase i. Since both phases exhibit an isotropic behavior, their stiffness tensor is characterized by two scalar parameters : the bulk modulus k_i and the shear modulus μ_i. The fibers bulk and shear moduli are both taken equal to 1 GPa, and the matrix bulk and shear moduli are taken equal to 10 kPa. $\boldsymbol{d_i}$ is the averaged second-order Eulerian strain rate tensor, and $\overset{\triangle}{\boldsymbol{\sigma}}_i$ is an objective derivative of the averaged second-order Cauchy stress tensor. The objective derivative is defined, for a quantity $\boldsymbol{a}$, as :

$$\overset{\triangle}{\boldsymbol{a}} = \dot{\boldsymbol{a}} + \boldsymbol{a} \cdot \tilde{\boldsymbol{\omega}} - \tilde{\boldsymbol{\omega}} \cdot \boldsymbol{a} \tag{2}$$

with $\tilde{\boldsymbol{\omega}}$ as the spin tensor defining the rotation of the point. Finally, uniform strain rate boundary conditions are considered, i.e. the RVE is subjected to uniform strain rate boundary conditions, applied in terms of velocity vectors $\dot{\boldsymbol{\xi}}$ at the boundary $\partial\Omega$ of the RVE :

$$\dot{\boldsymbol{\xi}}(\boldsymbol{x}) = \boldsymbol{D} \cdot \boldsymbol{x} \quad \forall \boldsymbol{x} \in \partial\Omega \tag{3}$$

with the dot as the time derivative, $\boldsymbol{\xi}$ as the displacement vector, $\boldsymbol{D}$ as the applied (macroscopic) Eulerian strain rate tensor and $\boldsymbol{x}$ as the location vector, labeling positions of microscopic points within and on the boundary of the RVE.

2.2 Homogenization methodology

The mechanical response and the morphology changes of the RVE are computed within the framework of continuum micromechanics under finite strains, by means of an incremental algorithm. For each increment of the applied velocity field, the local (microscopic) strain rate and vorticity tensors (respectively the symmetric and skew-symmetric parts of the microscopic velocity gradient) quantify the rate of deformation and of rotation of the different phases. As it can be derived from Eshelby's 1957 results [1], the microscopic velocity gradient within the inclusion is linearly related to the macroscopic loading applied at the boundary of the RVE. Semi-analytical expressions are derived for the linearity operators relating the applied macroscopic strain rate $\boldsymbol{D}$ to the microscopic vorticity tensor $\boldsymbol{\omega}_i$ (Eshelby fourth-order rotation tensor $\mathcal{R}_i$) and to the microscopic strain rate tensor $\boldsymbol{d}_i$ (Eshelby fourth-order strain concentration tensor $\mathcal{A}_i$) :

$$\boldsymbol{d}_i = \mathcal{A}_i : \boldsymbol{D} \quad (i \in \{f, m\}) \tag{4}$$

$$\boldsymbol{\omega}_i = \mathcal{R}_i : \boldsymbol{D} \quad (i \in \{f, m\}) \tag{5}$$

These relations quantify load-induced micro-configurational changes and allow to compute in each phase the local spin tensor $\tilde{\boldsymbol{\omega}}_{\boldsymbol{i}}$, its precise expression depending on the choice of the objective derivative according to (2). Then, the rate of rotation $\dot{\boldsymbol{e}}_j$ of the local base vectors $\boldsymbol{e}_j$ associated to the fibers is given by :

$$\dot{\boldsymbol{e}}_j = \tilde{\boldsymbol{\omega}}_{\boldsymbol{f}} \cdot \boldsymbol{e}_j \quad (j = \{r, \theta, \phi\}) \tag{6}$$

with $\tilde{\boldsymbol{\omega}}_{\boldsymbol{f}}$ as the local spin tensor in the fiber-like inclusions. For sake of simplicity, we here choose the Jaumann derivative with the spin tensor $\tilde{\boldsymbol{\omega}}_{\boldsymbol{f}}$ taken equal to the vorticity tensor $\boldsymbol{\omega}_f$. The microscopic stress rates are then computed by means of the local constitutive relations (1) and integrated over time. Finally, the macroscopic Cauchy stress $\boldsymbol{\Sigma}$ is determined by the stress average rule.

2.3 Loading paths : closed elastic strain cycles

We investigate different uniaxial and biaxial loading-unloading trajectories, and study the evolution of the morphology along these trajectories, the associated macroscopic responses and the absorption and release of elastic strain energy density.

We here focus on three trajectories, all starting from and returning to zero deformation state.

— Trajectory 1 : uniaxial tensile loading-unloading test along direction $\boldsymbol{e}_2$;
— Trajectory 2 : tensile loading along $\boldsymbol{e}_2$ followed by tensile loading along $\boldsymbol{e}_3$ (with maximum tensile strain along $\boldsymbol{e}_2$ maintained) and unloading successively along directions $\boldsymbol{e}_3$ and $\boldsymbol{e}_2$;
— Trajectory 3 : tensile loading along $\boldsymbol{e}_2$ followed by tensile loading along $\boldsymbol{e}_3$ (with maximum tensile strain along $\boldsymbol{e}_2$ maintained) and unloading successively along directions $\boldsymbol{e}_2$ and $\boldsymbol{e}_3$.

3 Results

The resulting micromechanical model for soft tissues allows to qualitatively reproduce the macroscopic response of soft tissues, with the progressive stiffening of the response being driven by the progressive reorientation of the fiber-like inclusions within the RVE, as seen on Figure 2a-b. Uniaxial loadings are fully reversible, and both the mechanical response (Figure 2b) and the orientations of the inclusions (Figure 2a) follow the exact inverse trajectory and return to their initial states. The response of the model to multiaxial loading cases is however more complex, and contrary to usual hyperelastic phenomenological models, the present micromechanical model allows reaching multiple stress states for the same deformation state, depending on the choice of the deformation trajectory. More precisely, the path dependence originates in the progressive micro-configurational changes occurring within the RVE and resulting in a history-dependent microscopic configuration of the fibers orientations. As a result, the reversibility of the mechanical response is preserved only if the unloading path follows the exact reverse path (Figure 2c & 2d) ; in this case, fibers return to their exact initial configuration and the macroscopic mechanical state is free of residual stresses. All the elastic energy stored in the system during loading is released during unloading. On the contrary when unloading follows a path different to the loading one, fibers do not reach their initial configuration although the final macroscopic deformation state is forced identical to the initial macroscopic configuration. As a consequence, the macroscopic

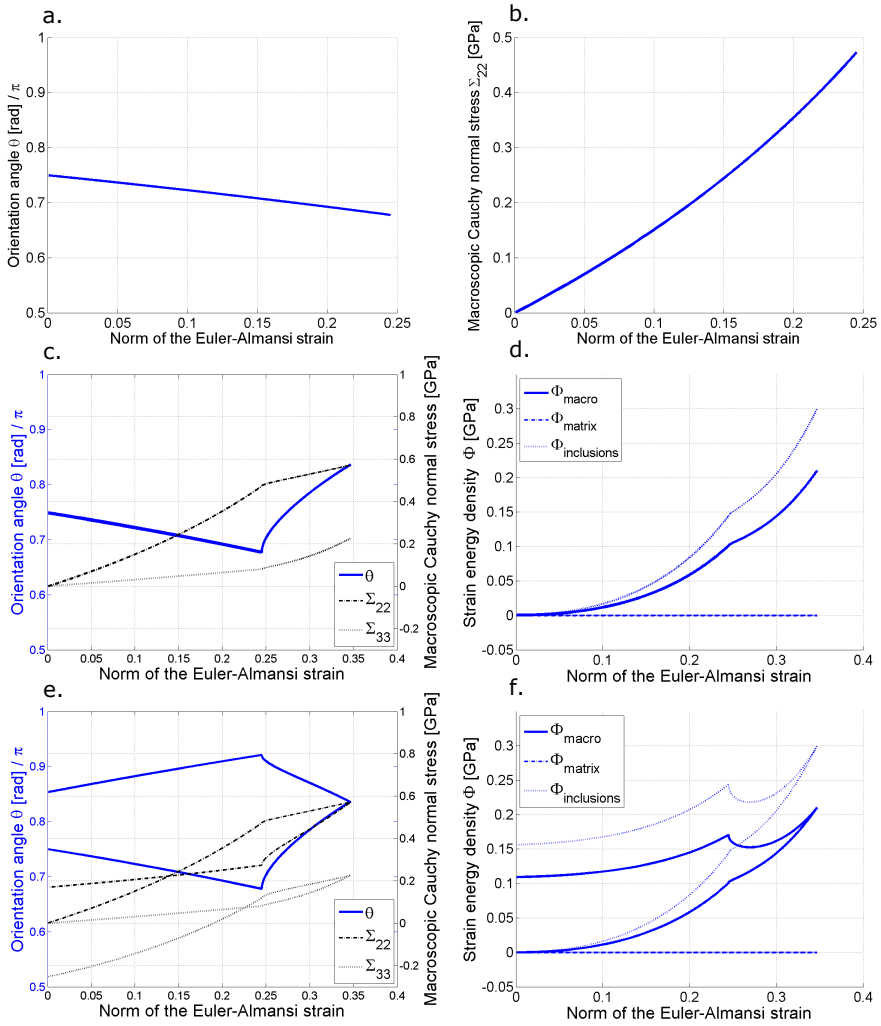

FIGURE 2 – *All quantities are represented as functions of the norm of the Euler-Almansi strain.* a. Trajectory 1 - Orientation angle θ of a given fiber family ; b. Trajectory 1 - macroscopic Cauchy stress. c. Trajectory 2 - Orientation angle θ of a given fiber family and macroscopic Cauchy stress ; d. Trajectory 2 - Macroscopic and microscopic strain energy densities ϕ ; e. Trajectory 3 - Orientation angle θ of a given fiber family and macroscopic Cauchy stress ; f. Trajectory 3 - Macroscopic and microscopic strain energy densities ϕ.

Cauchy stress does not return to zero, there is an insufficient release of absorbed elastic energy (observed hysteresis), resulting in final "frozen" elastic energy in the material as a consequence of the change in microstructure morphology (Figure 2e & 2f).

4 Conclusion

This is the first hypoelastic micromechanical model for soft tissues introducing a limited number of physical parameters. The modeled mechanical behavior exhibits path-dependence of the response and possible frozen elastic energy remaining in the system after complete unloading. This behavior originates in the micro-configurational changes occurring in the microstructure due to the application of loads and resulting in history-dependent configurations of fiber orientations. Future work will focus on the evolution of residual stresses after successive closed deformation loops, and the possible stabilization of residual stress accumulation, including the use of logarithmic rather than Jaumann-type stress rates, as the former prove to be fully consistent from kinematic as well as energetic viewpoints [11].

Acknowledgments

This material is based upon work supported by the ARC2 program of the Rhône-Alpes region (FR). The authors gratefully acknowledge travel funds provided through the 2015-2016 ÖAD-Campus France Hubert Curien project ♯33799NB.

References

[1] Eshelby J. D., The Determination of the Elastic Field of an Ellipsoidal Inclusion, and Related Problems, Proceedings of the Royal Society of London. Series A. Mathematical and Physical Sciences, 241(1226), 376–396 (1957)

[2] Gasser T., Ogden R., Holzapfel G., Hyperelastic modelling of arterial layers with distributed collagen fibre orientations, Journal of the Royal Society Interface 3, 15–35 (2006)

[3] Holzapfel G., Gasser T, A New Constitutive Framework for Arterial Wall mechanics and comparative study of material models, Journal of Elasticity 61, 1–48 (2000)

[4] Holzapfel G., Ogden R., Constitutive modelling of arteries, Proceedings of the Royal Society A 466, 1551–1597 (2010)

[5] Mooney M., A Theory of Large Elastic Deformation, Journal of Applied Physics, 11(9), 582-592 (1940)

[6] Mori, T., Tanaka, K., Average stress in matrix and average elastic energy of materials with misfitting inclusions, Acta Metal, 21 (5), 571–574 (1973)

[7] Morin C., Hellmich C., A multiscale poromicromechanical approach to wave propagation and attenuation in bone, Ultrasonics 54, 1251–1269 (2014)

[8] Ogden R., Large Deformation Isotropic Elasticity - On the Correlation of Theory and Experiment for Incompressible Rubberlike Solids, Proceedings of the Royal Society A, 326(1567), 565-584 (1972)

[9] Rivlin R., Large Elastic Deformations of Isotropic Materials. I. Fundamental Concepts, Philosophical Transactions of the Royal Society, 240(822), 459-490 (1948)

[10] Schrauwen J., Vilanova A. et al, A method for the quantification of the pressure dependent 3D collagen configuration in the arterial adventitia, Journal of Structural Biology 180 335–342 (2012)

[11] Xiao H., Bruhns O. T., Meyers A., Logarithmic strain, logarithmic spin and logarithmic rate, Acta Mechanica 124, 89-105 (1997)

[12] Zaoui A., Continuum Micromechanics : Survey, Journal of Engineering Mechanics 128(8), 808-816 (2002)